POLITECNICO DI TORINO
Repository ISTITUZIONALE

FIELD ORIENTED CONTROL OF IPM DRIVES FOR FLUX WEAKENING APPLICATIONS

Original
FIELD ORIENTED CONTROL OF IPM DRIVES FOR FLUX WEAKENING APPLICATIONS / Pellegrino, Gianmario; Armando, ERIC GIACOMO; Guglielmi, Paolo. - In: EPE JOURNAL. - ISSN 0939-8368. - STAMPA. - 20:(2010), pp. 50-57.

Availability:
This version is available at: 11583/2036288 since: 2017-11-03T00:55:37Z

Publisher:
EPE

Published
DOI:

Terms of use:

This article is made available under terms and conditions as specified in the corresponding bibliographic description in the repository

Publisher copyright
Taylor and Francis postprint/Author's Accepted Manuscript

(Article begins on next page)

20 April 2024

Field Oriented Control of IPM Drives for Flux Weakening Applications

Keywords

Adjustable speed drive, Control of Drive, Vector Control, Field-weakening control.

Abstract

Interior Permanent Magnet (IPM) drives are adapted to flux-weakening, then to constant power operation over a wide speed range. Most of the control strategies for IPM motor drives are based on the control of the current vector. Flux-weakening is obtained by proper current references, that are calculated according to the magnetic model of the motor. This approach needs the accurate characterization of the motor and it is sensitive to the inaccuracy and the variation of the model parameters. Moreover, in the case of a variable dc-link, an additional voltage loop is necessary to correct the current references values at different dc-link voltage levels. The direct control of the flux vector, in the stator flux oriented frame, is proposed here, with the aim of obtaining the constant voltage operation of the IPM motor drive in the flux weakening range by means of a very simple control algorithm. The proposed direct flux control is tested on an IPM motor drive designed for traction. The exploitation of the maximum torque in all the operating speed range is demonstrated. The control is also capable to adapt its flux and current set-points to different dc-link voltage levels with no need of additional voltage regulators. Discrete-time simulation and experimental results are presented and compared showing good accordance.

Introduction

Among variable speed AC drives, the IPM motor drives are particularly adapted to flux-weakening applications such as vehicle propulsion and machine tools, where a wide constant-power speed range is required [1, 2]. The flux weakening capability of an IPM motor depends on the motor design and it is a trade off between the rotor saliency and the permanent magnet quantity [3]. Once the IPM motor has been designed for having a high flux-weakening capability [4, 5], a proper control strategy is needed to obtain the maximum motor torque capability for a given inverter size (voltage and current limits). In other words, once the inverter and the motor are given, the control strategy must be able to exploit the inverter current and voltage limits completely. Space-vector control strategies for IPM motor drives are normally based on the control of the current vector in the dq frame, synchronous to the rotor [6, 7] . In those cases, field-weakening is obtained by adapting the current reference according to speed on the base of the motor magnetic model [8, 6]. This approach requires the accurate knowledge of the machine model and it is rather sensitive to the model parameters. Moreover, the current references are necessarily calculated for a determined dc-link voltage. In case the dc-link is not exactly constant like it happens with battery or fuel-cell supplied AC drives, an additional voltage loop is needed to correct the current reference vector [7, 9].

As usual for the control of Induction Motor (IM) drives, flux estimators and observers have been also proposed for IPM motor drives, in order to overcome the limitations of the current control in field-weakening operation [10, 11, 12]. For example, the flux amplitude is controlled by an exterior flux loop, like for Induction Motor drives [13, 14, 15], or the flux vector dq-components are controlled instead of the current components [10], e.g. the λ_d, i_q control proposed in [16].

The direct control of the flux is here proposed in the flux-oriented reference frame. Direct flux control has been rarely adopted. In [17, 18] it is proposed for for Synchronous Reluctance Machines, while in [19] and [20] for IPM motor drives. The use of the field-oriented frame is mutuated from the control of IM drives. The direct flux control proposed here has some aspects in common with the stator flux oriented control of IM drives (IM-SFOC), that has good performance in flux-weakening [21].

The proposed algorithm is very easy to implement and permits the exploitation of the current and voltage limits of the inverter with no need of reference look-up tables, that are difficult to calculate and that are stiffly related to a determined dc-link level. Also in case of a dc-link voltage spread, the direct-flux is capable of exploiting the available voltage completely with no particular modification.

The control is implemented for an IPM motor drive designed for light EV traction ($7kW@2800rpm$). The speed range is $2800 \div 10.000rpm$.

The IPM motor is of the PMASR type (Permanent-Magnet-Assisted Synchronous Reluctance) a definition that can be also found in [22].

IPM Motor Model

The magnetic curves of the IPM motor under test are reported in Fig.1-(b). Cross-saturation effects are evidenced by the spread of the λ_d and λ_q curves for different cross-current values. The saliency ratio of the motor is high, as demonstrated by the different slopes of $d-$ and $q-$ fluxes, while the permanent-magnet flux ($0.07Vs$ @ $i_d = i_q = 0$) is little respect to the d-axis flux ($0.35Vs$ is the rated d-flux). For this reasons, the motor can be referred to as a PMASR motor as already said: the choice of the (d,q) axes defined in Fig.1-(a) is unusual for IPM motors since it is the frame in use for Synchronous Reluctance machines. The typical IPM machine axes are indicated as (d',q') in Fig.1-(a).

The experimental model of Fig.1-(b) has been reported for having a precise idea of the machine under test, and will be also used here for outlining in detail the motor torque and speed capability at given inverter current and dc-link voltage.

However, for the sake of control implementation, the simplified magnetic model presented in the next subsection (2) will be adopted, with constant d and q inductances and no cross saturation term.

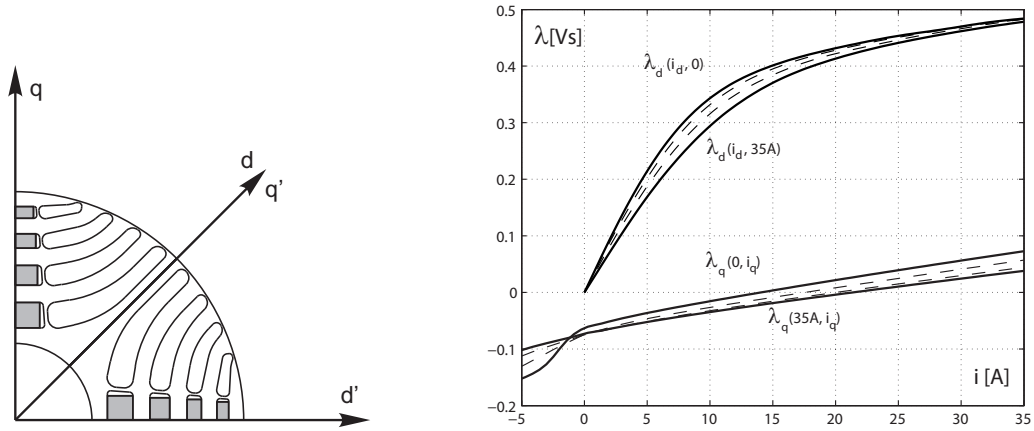

(a) Adopted (d,q) frame respect to standard IPM motor frame (d',q')

(b) Magnetic Characteristics

Figure 1: Definition of the (d,q) reference frame and experimental magnetic model of the motor.

Motor model in the dq synchronous frame

Apart for the different orientation of the axes (Fig.1-a), the rotating reference frame (d,q) is synchronous with the rotor. The IPM motor model in (d,q) is described by (1)-(3). According to the axes orientation, the PM flux is aligned to the q-axis and it is negative.

$$\bar{v}_{dq} = R \cdot \bar{i}_{dq} + \frac{d\bar{\lambda}_{dq}}{dt} + j \cdot \omega \bar{\lambda}_{dq} \tag{1}$$

$$\bar{\lambda}_{dq} = \begin{vmatrix} L_d & 0 \\ 0 & L_q \end{vmatrix} \cdot \bar{i}_{dq} - \begin{vmatrix} 0 \\ \lambda_m \end{vmatrix} \tag{2}$$

$$\frac{T}{3/2p} = \lambda_d i_q - \lambda_q i_d \tag{3}$$

Where p is the pole-pairs, R is the stator resistance, L_d, L_q are the inductances of maximum and minimum permeance axes, λ_m is the PM flux and T is the electromagnetic torque.

Motor model in the flux-oriented frame

The field oriented reference frame (f,τ), where f stands for $flux$ and τ stands for $torque$, is defined in Fig.2. The f-axis is oriented along the stator flux vector that is phase shifted by the angle δ with respect to the d-axis, where δ is the phase of the flux vector in the dq frame, according to (4).

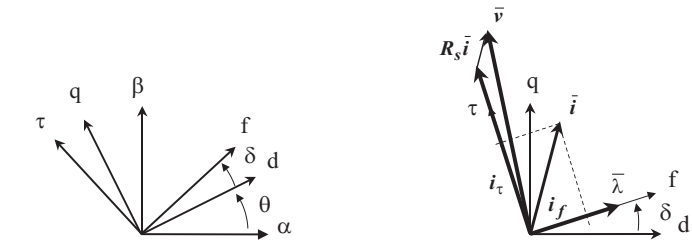

(a) $\alpha-\beta$: stator frame; $d-q$: rotor frame; $f-\tau$: flux frame

(b) Steady state vector diagram

Figure 2: Definition of the $f-\tau$ reference frame and IPM motor vector diagram.

$$\bar{\lambda}_{dq} = \lambda \cdot \begin{vmatrix} cos\delta \\ sin\delta \end{vmatrix} \tag{4}$$

In the new coordinates the two state variables λ and δ are decoupled between the f and τ components in the state equation (5).

$$\bar{v}_{f\tau} = R \cdot \bar{i}_{f\tau} + \frac{d}{dt} \begin{vmatrix} \lambda \\ 0 \end{vmatrix} + \lambda \cdot \begin{vmatrix} 0 \\ \omega + \frac{d\delta}{dt} \end{vmatrix} \tag{5}$$

$$\frac{T}{3/2p} = \frac{1}{L_q} \cdot \left\{ \left(1 - \frac{L_q}{L_d}\right) \cdot \lambda^2 \cdot \frac{sin2\delta}{2} + \lambda_m \lambda \cdot cos\delta \right\} \tag{6}$$

$$\frac{T}{3/2p} = \lambda \cdot i_\tau \tag{7}$$

where λ is the stator flux amplitude and δ is the phase angle with respect to the d axis. The torque expression (6) has been obtained by substituting (2) and (4) in (3).

The adoption of the field-oriented reference frame simplifies the voltage expression since the motor voltage is practically in quadrature with the machine flux, as evidenced in Fig.2-b: the management of the inverter voltage limit by means of the direct flux control in flux coordinates is very straightforward, as will be demonstrated in the following sections. Moreover, it is worthy to notice that the torque-current component i_τ introduced in (7), significantly simplifies the expression of torque: by means of this new couple of variables (λ, i_τ) the control of the motor torque is also simplified, as will be shown in the following.

Selection of the controlled variables: λ and i_τ

In the voltage equation (5), the two state variables are the flux amplitude and phase angle λ and δ. However, the expression of torque in λ, δ is quite complicate and achieving a linear and decoupled control of the torque by means of λ and δ is not straightforward (6). The control of the i_τ current component instead of δ permits the control of the torque by means of the simple and decoupled scheme presented hereafter. Moreover, the limitation of the motor current amplitude, according to the inverter maximum current, is easily obtained by the control of i_τ, as will be shown in the followings. The voltage equation in the new variables is reported in (8).

$$\frac{d}{dt} \begin{vmatrix} \lambda \\ i_\tau \end{vmatrix} \cong \begin{vmatrix} 1 & 0 \\ \frac{k}{L_q} & \frac{b}{L_q} \end{vmatrix} \cdot \begin{vmatrix} v_f \\ v_\tau - \omega\lambda \end{vmatrix} \tag{8}$$

where:

$$k = k(\delta) = \frac{1}{2}\left(1 - \frac{L_q}{L_d}\right) sin2\delta \tag{9}$$

$$b = b(\lambda, \delta) = \frac{L_q}{\lambda^2}\left(\frac{dT}{d\lambda}\right)_{\lambda = const} = \left(1 - \frac{L_q}{L_d}\right) cos2\delta - \frac{\lambda_m}{\lambda} sin\delta \tag{10}$$

The resistive drops have been disregarded in (8). The variable terms $b(\lambda,\delta)$ and $k(\delta)$ are two functions of the machine magnetic state. This means that the control of the i_τ current component will be influenced by the actual amplitude and phase of the machine flux as explained in the next section.

Direct flux, field oriented control scheme

The proposed control scheme is reported in Fig.3. The flux reference λ^* is determined by the requested torque according to the linear control law (11). Once the reference flux is set, the i_τ^* value is calculated coherently with the torque expression (7).
The *flux weakening* block limits the reference flux above the base speed ($\omega > \omega_A$), before the reference i_τ^* is calculated. The limitation block on i_τ^* ensures the respect of the inverter current limit I_{max}.

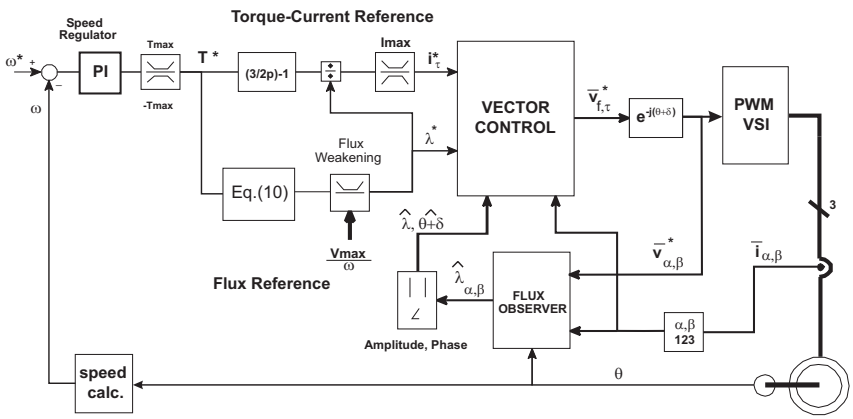

Figure 3: Proposed Control Scheme in the field oriented frame (f,τ). The controlled variables are λ, i_τ.

Vector Control block.

The λ and i_τ regulators are of the Proportional-Integral (PI) type. According to (8), the flux amplitude can be controlled by means of the v_f voltage, with no influence of the τ components. The flux loop response is very fast: apart from the limitation due PWM time discretization, the flux bandwidth is limited only by the dynamics of the flux estimator. With most of the flux observers in the literature bandwidths in the order of the kHz or more are possible.
The control of the i_τ current is obtained through the v_τ voltage, but with less ideal properties respect to λ. First of all, there is an interaction with the flux loop given by the v_f and $\omega\lambda$ terms in (8). This interaction is dynamically tackled by the fast response of the proportional i_τ regulator. The integrative regulator then compensates the v_f disturbance at steady state, while the back-EMF term $\omega\lambda$ must be conveniently compensated in feed-forward. The dynamic response of the i_τ regulator strongly depends on the factor $b(\lambda,\delta)$ defined in (10) that varies with the working point of the motor. Since b is not constant, a constant proportional gain will give different closed-loop response of i_τ for different operating points. For a stable and well damped response of the regulator, it is suggested to choose the proportional gain with reference to the best-case condition, that is $b = b_{max}$. The bandwidth of i_τ will be lower than the rated value $(\omega_b)_\tau$ since normally $b < b_{max}$.

Maximum Torque per Voltage trajectory ($b = 0$).

The factor b assumes negative values in part of the flux plane. In case of $b < 0$ the i_τ control would be unstable, due to positive feedback. The $b = 0$ curve is the border of torque instability, and it is reported in Fig.4-b for the drive under test. According to the definition given in (10), $b = 0$ means that the torque derivative with respect to flux phase angle is null. This trajectory coincides with the field-weakening region II or the Maximum Torque Per Voltage (MTPV) trajectory. It corresponds to deep flux weakening conditions that occurs at very high speed, at least for the drive under test. The MTPV curve is the optimal control trajectory for maximum torque at high speed. The instability due to $b < 0$ does not occur if the MTPV trajectory is respected. In the proposed control the constraint $b = 0$ is fulfilled by proper limitation of the i_τ reference value. In the following it will be shown that $b = 0$ falls out of the speed range of the drive under test and this limitation will not be implemented here.

Flux reference at low speed

The flux reference is set by means of the linear law (11). The minimum flux set at no load equals the permanent magnets flux λ_m. Then the flux reference is increased proportionally with the torque. The flux reference λ_{nom} at rated torque T_{nom} is chosen according to the Maximum Torque Per Ampere curve shown in Fig.4 (MTPA - point A), as will be better explained in the followings.

$$\lambda^* = \lambda_m + |T^*|/T_{nom} \cdot (\lambda_{nom} - \lambda_m) \tag{11}$$

Flux Weakening

The flux reference is limited according to the actual speed and the inverter maximum voltage by means of the simple relationship (12), where the resistive drops are not considered.

$$\lambda^* \leq \frac{V_{max}}{|\omega|} \tag{12}$$

In case the limit V_{max} is not a constant value (e.g. battery supplied drive for traction), the flux weakening block is calculated according to the measured dc-link voltage (13).

$$\lambda^* \leq \frac{V_{dc}}{\sqrt{3} \cdot |\omega|} \tag{13}$$

where V_{dc} is the measured dc-link voltage and $alpha$ is a constant term, minor or quasi-equal to the unity, that relies for the voltage margin left by the designer for the dynamics of the flux and current regulators. In the presented experimental results $\alpha = 0.90$ has been adopted. The resistive term can be also considered in the flux weakening law by small modification of (12), but it is negligible in most of cases at high speed.

Maximum current limit.

The I_{max} saturation block in Fig.3 limits i_τ^* according to the amplitude of the measured current (14).

$$i_\tau^* \leq \sqrt{I_{max}^2 - i_f^2} \tag{14}$$

where i_f is the current component in phase with the flux (5).

Maximum Torque Per Voltage limit

The MTPV or $b = 0$ limit curve is out of the operating region of the IPM motor drive under test, according to the speed range specified in Table I in the Appendix. As evidenced in Fig. 4, the MTPV zone would occur above 17000rpm, while the maximum speed of the drive is $10000rpm$. In case MTPV is exploited, a further limitation of the i_τ reference would be necessary.

Flux Observer

The control performance rely on the accuracy of the flux observer. The flux observer scheme adopted here is the one proposed in [10], based on the motor magnetic model at low speed and on back-EMF integration at high speed. The motor model adopted in the flux observer is the simplified magnetic model reported in (1). The L_d value corresponds to the apparent value at rated machine flux, that is the saturated value. Despite the model inaccuracy, the response of the observer is fast at any speed and the sensitivity to motor's parameters is very weak:

- at very low speed, far below the field weakening region, the simplified magnetic model introduces an error in the flux module and orientation estimations. This errors can produce an error in the controlled torque, that is usually compensated by the speed loop, but no effect at rated torque and current since the rated L_d value has been implemented in the flux observer;
- as the speed increases the flux estimation error vanishes due to the back-EMF contribution. Above the base speed ω_A, the flux estimation is normally correct;
- the detuning of motor resistance has little effect since the back-EMF scheme operates at high speed where the resistive term is negligible;
- apart from the PM flux term, the magnetic model is practically insensitive to temperature. The PM flux term here is small respect to the total flux, as usual for IPM machines of the PMASR type.

Drive operation limits in flux coordinates

In case the IPM motor drive is current controlled, the maximum-torque control in field weakening relies on the current vector trajectory represented in Fig.4-a, that referes to the dq-current frame, for the drive under test. The trajectory is referenced by the letters $A \rightarrow B \rightarrow C$. It must be remarked, again, that the dq axes are rotated by 90 degrees clockwise with respect to the ones usually adopted for IPM motors. The trajectory $A \rightarrow B \rightarrow C$ is reported in the flux diagram (λ_d, λ_q).
With reference to current and flux planes in Fig.4, constant current contours are circles in the current plane (a) and ellipses with a vertical offset in the flux plane (b). Analogously, constant flux (i.e. voltage) contours are offset ellipses in the current plane and circles in the flux plane. The trajectory $A \rightarrow B \rightarrow C$ is briefly described in the followings, independently on type of control (current vector control or direct flux control). The inverter ratings are summarized by the current and voltage limits I_{max} and V_{max},referenced in Table I in the Appendix.

- Point A (speed $0 \div \omega_A$): it is the intersection between the Maximum Torque Per Ampere Curve and the I_{max} circle. Nominal torque and flux follow: $T_{nom} = 20Nm, \lambda_{nom} = \lambda_A = 0.363Vs$, as well as base speed $\omega_A = 2700rpm$, calculated at (V_{max}, λ_A).
- Trajectory $A \rightarrow B$ (speed $\omega_A \div \omega_B$): is the current and voltage-limited region, along the I_{max} circle. It is the region from the base speed ω_A to ω_B that is calculated according to V_{max} and λ_B. For the drive under test $\lambda_B = 0.065Vs$ and $\omega_B = 17000rpm$ is greater than maximum operating speed.
- Trajectory $B \rightarrow C$ (speed $\omega_B \div \infty$): is the voltage-limited region. The drive operates on the MTPV curve ($b = 0$), virtually with no upper speed limit.

The maximum torque and power performance corresponding to Fig.4-a and-b diagrams is then reported in Fig. 5.

Simulated and Experimental results

The IPM motor under test is rated $7kW$ in the speed range $2700 \div 10000$ rpm. The direct field-oriented control is tested in simulation (Matlab Simulink) and then implemented on a floating point micro-controller (ADSP 21060 sharc). The use of C- SFunctions in Simulink, allows the portability of the control code from simulation to experimental implementation. This approach is very powerful for development purposes, and results in simulations that match very well the experimental data. Nevertheless, the algorithm is suitable for fixed-point implementation on a low-cost DSP, since it's simple and straightforward as demonstrated along the paper.
The drive response to a speed step command from zero to 8000rpm at no load is shown in Fig.6. The full exploitation of maximum voltage is evidenced.
The transient trajectory of the flux vector, both in motoring and braking, is shown in Fig.7, for a step response from zero to maximum speed and back to zero. In flux weakening, the flux follows the $A \rightarrow B$ trajectory introduced in Fig.4-b, along the I_{max} ellipse . The simulation points out a small error on the observed flux, due to time-discretization: the observed flux lags or leads the actual flux by the sampling

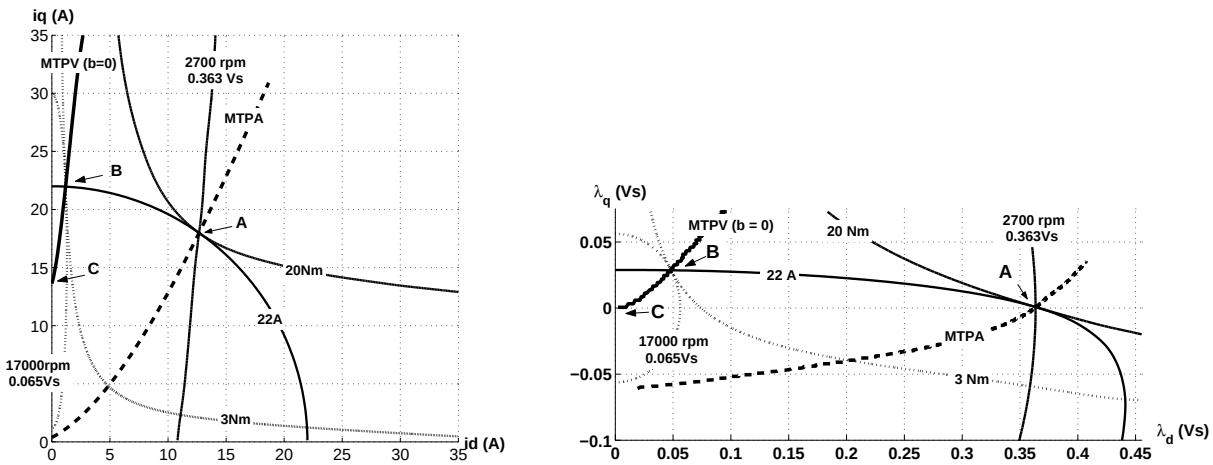

(a) Current Coordinates

(b) Flux Coordinates

Figure 4: Current and flux trajectories for maximum torque control.

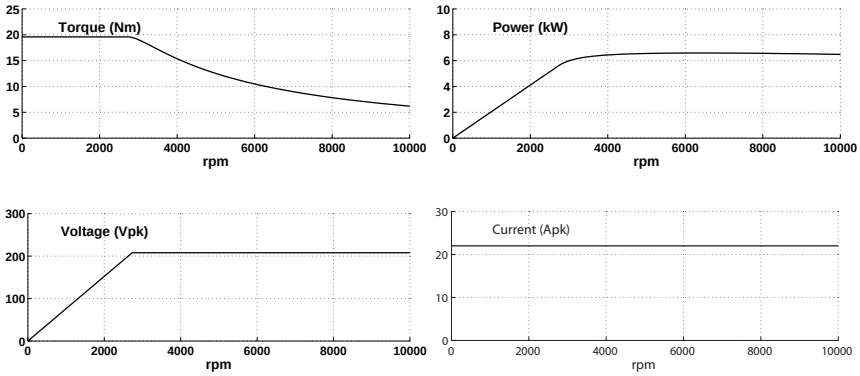

Figure 5: Maximum torque and power performance of the IPM motor drive under test according to the inverter maximum ratings reported in the Appendix.

period (100) in motoring and braking operation respectively. The orientation error causes a small reduction of the actual torque with respect to the reference one, while the flux amplitude error reflects on the motor voltage value in flux weakening. Both the effects have no practical impact on the IPM motor drive performance. The current limit is still exactly obtained since the I_{max} strategy is based on the measured current.
The flux vector trajectory from zero to maximum torque in quasi-stationary conditions is shown in Fig.8. The flux trajectory corresponds to the linear control law (11). In comparison with the MTPA curve reported in Fig.4-b, torque values are obtained by a smaller flux amplitude then by a higher current value that could be minimized by the adoption of the MTPA control law. The linear control law (11) has been adopted here for its simplicity. Nevertheless, at rated torque MTPA and (11) converge to point A where nominal torque $T_{nom} = 20Nm$ is obtained.

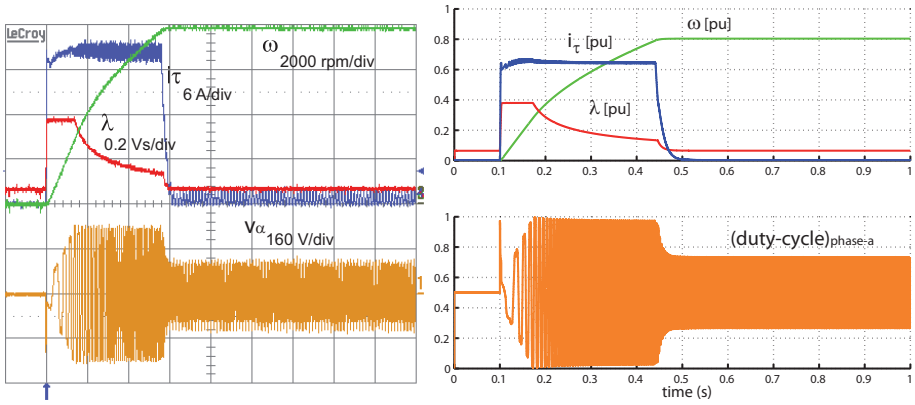

(a) Experimental. (10V/1pu , 0.1s/div)

(b) Discrete-time simulation

Figure 6: Drive response to speed step command 0 → 8000. Scale factor for plot (b): v_α^*: 230 V/pu, ω: 10000 rpm/pu, $\widehat{\lambda}$: 1 Vs/pu, i_τ: 30 A/pu.

Conclusions

The direct flux control of an IPM motor drive with large flux weakening capability has been proposed in the field-oriented reference frame. Experimental tests have been carried out on a drive for EV traction, rated 7kW. The exploitation of the current and voltage limits of the inverter is obtained by means of a simple control algorithm. The method is robust toward flux estimation errors at low speed, while flux estimation is accurate in the flux weakening region with any flux observer based on back-EMF integration. The respect of the voltage limit is obtained also with large variations of the dc-link. The control strategy is particularly adapt to motor drives designed for electrical and hybrid traction, with a large constant power speed range and a battery of fuel-cell power supply. Due to its simplicity, the algorithm is suitable for implementation on a low-cost, fixed-point DSPs.

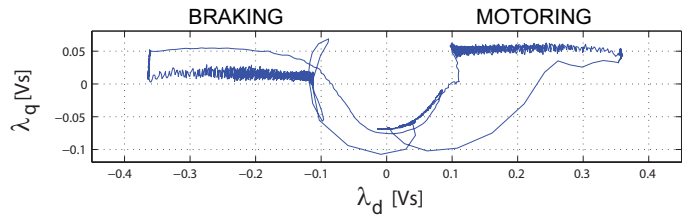

(a) Experimental.

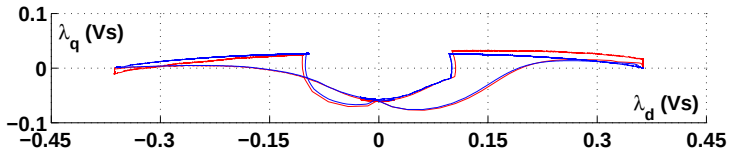

(b) Discrete-time simulation. Red: actual flux; blue: observed flux.

Figure 7: Flux trajectory in transient at full power, full speed. Motoring: step $0 \rightarrow 10000rpm$. Braking: step $0 \rightarrow 10000rpm$.

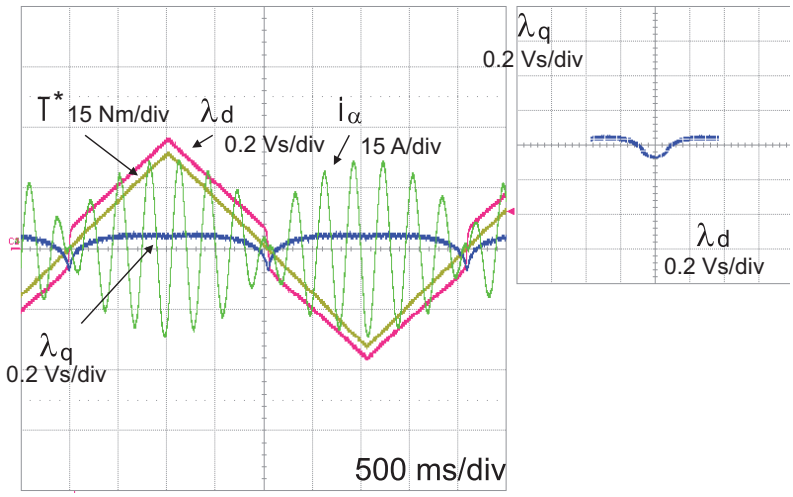

(a) Experimental Test. (10V/1pu)

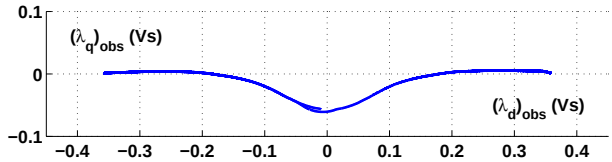

(b) Discrete-time simulation

Figure 8: Quasi-stationary flux path over the torque range $[-T_{max}, T_{max}]$.

APPENDIX: IPM motor drive data.

The motor under test is designed for light electrical traction. The motor and inverter ratings are summarized in Table I.

References

[1] T.M.Jahns, G.B.Kliman, and T.W.Neumann. Interior permanent magnet synchronous motors for adjustable speed drives. *IEEE Transactions on Industry Applications*, IA-22(4):678–690, 1986.

[2] A.Fratta, A.Vagati, and F.Villata. On the evolution if ac machines for spindle drives applications. *IEEE Transactions on Industry Applications*, 28(5):1081–1086, 1992.

Table I: IPM drive ratings at $25°C$.

MOTOR DATA			
Power	P	kW	7
Base Speed	ω_A	rpm	2700
Max Speed	ω_{max}	rpm	10000
Stator resistance	R	Ω	0.3
Inertia (Motor)	J	kg m^2	4.5 10^{-3}
INVERTER DATA			
Current	I_{max}	Apk	22
Voltage (star)	V_{max}	Vpk	210

[3] W.L.Soong and T.J.E.Miller. Field-weakening performance of brushless synchronous ac motor drives. In *Proc. of IEE Electr. Power Appl.*, volume 141, pages 331–340, 1994.

[4] A.Fratta, A.Vagati, and F.Villata. Design criteria of an ipm machine suitable for field-weakening operation. In *Proc. of International Conference on Electrical Machines*, pages 1059–1065, 1990.

[5] N. Bianchi, S. Bolognani, and B.J. Chalmers. Salient-rotor pm synchronous motors for an extended flux-weakening operation range. *Industry Applications, IEEE Transactions on*, 36(4):1118–1125, Jul/Aug 2000.

[6] S.Morimoto, T.Ueno, M.Sanada, Y.Takeda, and T.Hirasa. Variable speed drive system of interior permanent magnet synchronous motors for constant power operation. In *Proc. of IEEE Power Conversion Conference*, pages 402–407, 1993.

[7] J.Kim and S.Sul. Speed control of interior permanent magnet synchronous motor drive for the flux weakening operation. *IEEE Transactions on Industry Applications*, 33(1):43–48, 1997.

[8] S.R. Macminn and T.M.Jahns. Control techniques for improved high-speed performance of interior pm synchronous motor drives. *IEEE Transactions on Industry Applications*, 27(5):997–1004, 1991.

[9] J. Wai and T.M.Jahns. A new control technique for achieving wide constant power speed operation with an interior pm alternator machine. In *Proc. of IEEE Industry Applications Society Annual Meeting*, volume 2, pages 807 – 814, 2001.

[10] A.Vagati, M.Pastorelli, G.Franceschini, and V.Drogoreanu. Digital observer-based control of synchronous reluctance motors. In *Proc. of IEEE Industry Applications Society Annual Meeting*, volume 1, pages 629 – 636, 1997.

[11] Kyeong-Hwa Kim, Se-Kyo Chung, Gun-Woo Moon, In-Cheol Baik, and Myung-Joong Youn. Parameter estimation and control for permanent magnet synchronous motor drive using model reference adaptive technique. *Industrial Electronics, Control, and Instrumentation, 1995., Proceedings of the 1995 IEEE IECON 21st International Conference on*, 1:387–392 vol.1, Nov 1995.

[12] Y.Jeong and S.K.Sul. Adaptive flux observer with on-line inductance estimation of an ipmsm considering magnetic saturation. In *Conf.Rec.IEEE-PESC*, pages 2467–2473, 2005.

[13] Sang-Hoon Kim and Seung-Ki Sul. Maximum torque control of an induction machine in the field weakening region. *Industry Applications, IEEE Transactions on*, 31(4):787–794, Jul/Aug 1995.

[14] F. Briz, A. Diez, M.W. Degner, and R.D. Lorenz. Current and flux regulation in field-weakening operation [of induction motors]. *Industry Applications, IEEE Transactions on*, 37(1):42–50, Jan/Feb 2001.

[15] Myoung-Ho Shin, Dong-Seok Hyun, and Soon-Bong Cho. Maximum torque control of stator-flux-oriented induction machine drive in the field-weakening region. *Industry Applications, IEEE Transactions on*, 38(1):117–122, Jan/Feb 2002.

[16] P.Guglielmi, M.Pastorelli, G.Pellegrino, and A.Vagati. Position sensorless control of permanent-magnet-assisted synchronous reluctance motor. *IEEE Transactions on Industry Applications*, 40(2):615 – 622, 2004.

[17] H.F.Hofmann, S.R.Sanders, and A.EL-Antably. Stator-flux-oriented vector control of synchronous reluctance machines with maximized efficiency. *IEEE Transactions on Industrial Electronics*, 51(5):1066–1072, 2004.

[18] S.P.Das and A.K.Chattopadhyay. Observer-based stator-flux-oriented vector control of cycloconverter-fed synchronous motor drive. *IEEE Transactions on Industry Applications*, 33(4):943–955, 1997.

[19] M.Bilewski, A.Fratta, L.Giordano, A.Vagati, and F.Villata. Control of high-performance interior permanent magnet synchronous drives. *IEEE Transactions on Industry Applications*, 29(2):328–336, 1993.

[20] Liu Qinghua, A.M. Khambadkone, and M.A. Jabbar. Direct flux control of interior permanent magnet synchronous motor drives for wide-speed operation. *Power Electronics and Drive Systems, 2003. PEDS 2003. The Fifth International Conference on*, 2:1680–1685 Vol.2, Nov. 2003.

[21] X.Xu and D.Novotny. Selection of the flux reference for induction machine drives in the field weakening region. *IEEE Transactions on Industry Applications*, 28(6):1353 – 1358, 1992.

[22] S. Morimoto, M. Sanada, and Y. Takeda. Performance of pm assisted synchronous reluctance motor for high efficiency and wide constant power operation. *Industry Applications Conference, 2000. Conference Record of the 2000 IEEE*, 1:509–514 vol.1, 2000.

[23] S.Morimoto, Y.Takeda, T.Hirasa, and K.Taniguchi. Expansion of operating limits for permanent magnet motor by current vector control considering inverter capacity. *IEEE Transactions on Industry Applications*, 26(5):678–690, 1990.

[24] N.Bianchi and S.Bolognani. Magnetic models of saturated interior permanent magnet motors based on finite element analysis. In *Proc. of IEEE Industry Applications Society Annual Meeting*, volume 1, pages 27 – 34, 1998.

[25] N.Bianchi and S.Bolognani. Unified approach to the analysis and design of an ac motor drive for flux-weakening operations. In *Proc. of IEEE Industry Applications Society Annual Meeting*, volume 1, pages 95 – 102, 1998.

[26] M.F.Rahman, L.Zhong, and K.W.Lim. A direct torque controlled interior permanent magnet synchronous motor drive incorporating field weakening. *IEEE Transactions on Industry Applications*, 34(6):1246 – 1253, 1998.

[27] S. Morimoto. Ipm vector control and flux weakening. In *TUTORIAL COURSE NOTES - Design, Analysis, and Control of Interior PM Synchronous Machines - IEEE Industry Applications Society Annual Meeting*, 2004.

[28] B.Stumberger, G.Stumberger, D.Dolinar, A.Hamler, and M.Trlep. Evaluation of saturation and cross-magnetization effects in interior permanent-magnet synchronous motor. *IEEE Transactions on Industry Applications*, 39(5):1264 – 1271, 2003.

[29] Z. Xu and M.F. Rahman. An improved stator flux estimation for a variable structure direct torque controlled ipm synchronous motor drive using a sliding, observer. *Industry Applications Conference, 2005. Fourtieth IAS Annual Meeting. Conference Record of the 2005*, 4:2484–2490 Vol. 4, Oct. 2005.

[30] T.J.E.Miller, M.Popescu, C.Cossar, and M.McGilp. Performance estimation of interior permanent-magnet brushless motors using the voltage-driven flux-mmf diagram. *IEEE Transactions on Industry Applications*, 42(7):1867 – 1872, 2006.

[31] G. Pellegrino, E. Armando, and P. Guglielmi. Field oriented control of ipm drives for optimal constant power operation. *Power Electronics and Applications, 2007 European Conference on*, pages 1–10, Sept. 2007.